

Solid-state ^1H n.m.r. studies of polypropylene

Dilek Dadayli*, Robin K. Harris, Alan M. Kenwright†, Barry J. Say and M. Maral Sünnetçioğlu‡

IRC in Polymer Science and Technology, University of Durham, South Road, Durham DH1 3LE, UK

(Received 11 November 1993; revised 14 February 1994)

Two samples of isotactic polypropylene (PP), with different treatment histories, were studied by carrying out a number of proton n.m.r. measurements, namely free induction decay (FID) and spin-lattice relaxation in both the laboratory and rotating frames. The results were subjected to detailed mathematical analysis, and are shown to yield information about the domain structure and intrinsic relaxation parameters. Inversion-nulled FID analysis shows that the samples contain a spatially resolved distribution of crystallinities, which is responsible for bi-exponential spin-lattice relaxation.

(Keywords: ^1H n.m.r.; polypropylene; free induction decay)

INTRODUCTION

Motional heterogeneity and morphology are important parameters for determining the macroscopic physical properties of semicrystalline homopolymers. The study of both the motional characteristics of the crystalline and amorphous phases, and their spatial distribution, is therefore of considerable interest to polymer scientists.

The use of wide-line ^1H n.m.r. techniques in such studies has a long history, dating back to the pioneering work of Wilson and Pake¹. Considerable progress has been made both in experimental techniques for relaxation measurements, and in data analysis methods (particularly as applied to lineshape/free induction decay (FID) analysis). In this work, we present results that have been obtained on samples of isotactic polypropylene extracted from industrial plant at different stages in the production process. We make use of a combination of classical relaxation techniques (^1H T_1 and $T_{1\rho}$), and analysis of the on-resonance FID to characterize the samples, and we show that this combination provides a powerful way of extracting information about the intrinsic relaxation behaviour of the crystalline and amorphous regions that are present in the sample. We also find that our results point to a spatially non-uniform distribution of percentage crystallinities within the samples.

EXPERIMENTAL

Samples

Samples of isotactic polypropylene (PP) were obtained from ICI plc, at two different stages in its manufacture. The first sample was extracted at a point immediately

after formation of the polymer; this sample is referred to as 'powder'. The second sample was extracted at a later stage in the process, after this powder had been extruded; this sample is referred to as 'granules'. The time interval between extracting the two samples was chosen as nearly as possible such that the two samples came from the same batch of bulk polymer. Therefore, the samples form a matched pair representing the same material at different stages in the manufacturing process. All the experiments reported were run over a relatively short time span (approximately two weeks) some five months after the samples were first collected, so that the relatively rapid change in percentage crystallinity which is observable in 'fresh' polypropylene at ambient temperature ('thermal ageing') had effectively stopped.

Measurements

Measurements were carried out at 60 MHz using a custom-built instrument which has been described elsewhere². All measurements were performed at a regulated temperature of 313 K. This is important since the strong variation of relaxation behaviour with temperature in polypropylene at around room temperature has been well documented³. The 90° pulses were of 2 μs duration, and the spin-lock field for the $T_{1\rho}$ measurements was 40 kHz. The 'solid echo'⁴ was used in the detection stage of all measurements, in an effort to overcome the effects of the dead-time, with an echo delay of 10 μs . Alternation of the phase of the echo pulse, while holding the phase of the read pulse constant, was employed, in addition to the normal phase cycling, to minimize any residual effects due to receiver overload.

Data analysis

The data were analysed using non-linear, least-squares fitting software written by us, employing both Simplex⁵ and Levenberg–Marquardt⁶ algorithms. The sum of squares of the residuals was compared to an

*Present address: Department of Physics, Zonguldak Karaelmas University, 67100 Incivez, Zonguldak, Turkey

†To whom correspondence should be addressed

‡Present address: Department of Physics Engineering, Hacettepe University, 06532 Beytepe-Ankara, Turkey

independent measurement of the noise to determine a measure of the 'goodness of fit', Q^7 . In addition, both the residuals, and their integral, were displayed to highlight any systematic deviations in the fit. A floating baseline was included as a fitting parameter where appropriate.

In the cases of T_1 and $T_{1\rho}$, the form of the relaxation curve is well understood, and is expected to be either an exponential, or a sum of exponential components. In these cases, interactive graphical methods were used to generate initial estimates for the non-linear least-squares optimization.

In the case of the on-resonance FID, the problem is rather more complicated, since the overall form of the FID is the sum of the components arising from the crystalline and amorphous phases, and the theoretical form of these components is not readily accessible. The problem of analysing the FID, or correspondingly the lineshape, of such a system dates back to the initial observations of Wilson and Pake¹, and has been the principal limitation of this analytical method. The history of this problem and the various functions which have been tried has recently been reviewed⁸. In this work we have represented the rapidly decaying portion of the FID by a Gaussian-broadened sinc function. This function was first suggested by Abragam⁹ as a phenomenological expression of the ^{19}F FID of CaF_2 , and has subsequently been found to be a good representation for the FID from other regular, crystalline lattices. In the present context, we believe it represents the signal arising from the crystalline regions of the sample. The remainder of the signal, which we believe arises from the amorphous regions of the sample, is represented as the sum of one or two exponential components plus a Weibullian¹⁰ component ($e^{-(t/T_2)^n}$). The Weibullian ranges between a Lorentzian ($n=1$) and a Gaussian ($n=2$). Although there is no direct theoretical justification for this choice of functions, it is worth noting that the sum of a Weibullian and one or two exponentials can well represent the theoretical expression derived by Breton¹¹ for the FID of amorphous polyethylene above its T_g , which has in turn been shown to be a satisfactory representation of the FIDs from polyethylene melts over a range of temperatures¹². Therefore, the use of this combination of functions to represent the signals from the amorphous regions of the samples is fully consistent with our theoretical understanding of the FID function which is to be expected in such polymeric materials.

Obviously, the problem of non-linear least-squares optimization of a function with so many parameters is ill-conditioned, and is likely to be prone to local minima. Nevertheless, repeated measurements and multiple fits

starting from slightly different 'guesses' gave reasonably consistent convergence, with residuals approaching statistical significance. The results quoted subsequently are the mean values obtained from several independent determinations.

RESULTS AND DISCUSSION

The results of analysing the on-resonance FID of each of the samples, in terms of four components, is presented in *Table 1*, and a representative breakdown of the early part of FID into the component functions is shown in *Figure 1*. During the course of this work, it was found that the results from this type of analysis depended to a significant extent on the value used for the delay in the solid-echo sequence. Although it is known that there should be some change in the relative intensities of the various components as a function of the echo delay, it has previously been assumed⁴ that, for short delay values, the shape of the decay side of the echo was a true representation of the shape of the FID. In this case, we found not only changes in the relative intensity, but also changes in the 'shape' parameters (particularly for the Abragamian), as a function of the echo delay. For this reason, the shortest practicable inter-pulse spacing ($10\ \mu\text{s}$)

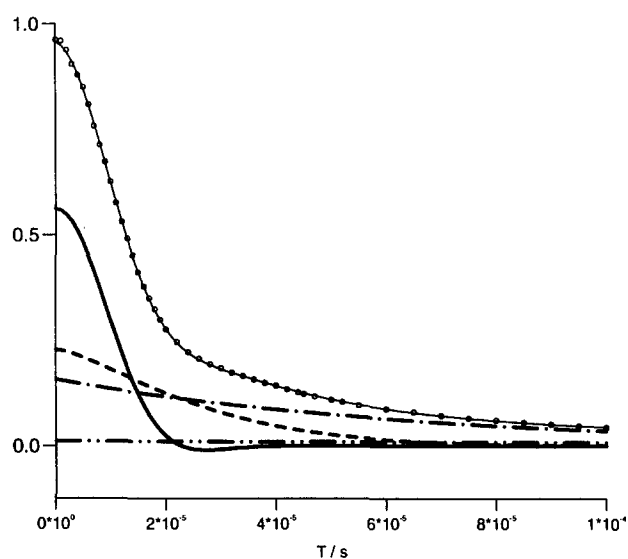


Figure 1 Example of free induction decay analysis for polypropylene granules, where the circles are the experimental points and the line through them represents the theoretical curve obtained by fitting. The separate components are: heavy solid line, Abragamian; dashes, Weibullian; remaining lines, the two exponentials. The vertical scale is in arbitrary units

Table 1 Results of FID analysis for polypropylene powder and granules

Form	Abragamian ^a			Weibullian ^b			Exponential 1		Exponential 2	
	%	T_c (μs)	ν (kHz)	%	T_c (μs)	n	%	T_c (μs)	%	T_c (μs)
Powder	52	18.4	21.6	29	29.6	1.34	15	72.6	4	382
Granules	61	19.0	22.0	22	28.2	1.40	16	57.1	2	241

$$^a M_t = M_o \frac{\sin 2\pi\nu t}{2\pi\nu t} \exp\left[-\left(\frac{t}{T_c}\right)^2\right]$$

$$^b M_t = M_o \exp\left[-\left(\frac{t}{T_c}\right)^n\right]$$

Table 2 Analysis of T_1 data obtained for polypropylene powder and granules

Form	One-component fit (s)	Two-component fit (s)	Population-weighted average (s)
Powder	0.46	0.65 (38%) 0.34 (62%)	0.42
	0.45	0.50 (80%) 0.27 (20%)	0.42
	0.46	0.50 (82%) 0.23 (18%)	0.42
Granules	0.50	0.54 (81%) 0.33 (19%)	0.48
	0.50	0.63 (38%) 0.43 (62%)	0.48
	0.50	0.57 (61%) 0.38 (39%)	0.48

was used in order to minimize any systematic distortion of the results.

Assuming that the signal represented by the Abragamian component arises from the crystalline regions of the sample, we can see from *Table 1* that the overall crystallinity of the material increases on conversion from powder to granules, i.e. the polypropylene is annealed during the extrusion process.

We next looked at the T_1 behaviour of the two samples. In both cases, we found that the T_1 relaxation deviated significantly from a single exponential process, and that substantially better fits were obtained by using a sum of two exponentials. However, the time constants for the two exponentials differed by less than a factor of two in each case, and so the covariance between parameters was too high for fitting to give reliable values for the individual components, particularly the populations. This sort of behaviour has been observed previously¹³, but its origin has remained unclear. We will return to this point later.

The problem of extracting reliable values for the individual parameters in a two-component fit is illustrated in *Table 2*, which gives the results of one- and two-component fits to the data from three separate determinations of T_1 , for both powder and granules. Although the results of the two-component fits seem to vary widely in both cases, calculation of a population-weighted 'average' value, i.e. the inverse of the population-weighted rate average, where the latter is given by:

$$\frac{1}{T_{1av}} = \left(\frac{P_S}{T_{1S}} + \frac{P_L}{T_{1L}} \right) / (P_S + P_L)$$

where S and L represent the short and long components, respectively, shows, in each case, remarkable consistency. It should also be noted that this weighted average value is significantly different from the result obtained from the (poorer) one-component fit.

This weighted average value is itself useful, since it can be shown (see Appendix) that for any multiregion system coupled by spin-diffusion, whose observed relaxation behaviour can be properly represented as a sum of exponentials, the population-weighted average of the observed relaxation components is equal to the population-weighted average of the intrinsic relaxation times

in the different regions. Since we have two samples with different percentage crystallinities, as determined by FID analysis, then if we assume a two-region model in each sample, and further assume that the intrinsic relaxation properties of the crystalline and amorphous regions are the same in both samples, we can then solve a set of simultaneous equations to obtain values for these intrinsic relaxation properties. When this is done using the percentage crystallinities reported in *Table 1*, and the mean of the population-weighted averages reported in *Table 2*, we find an intrinsic T_1 for the amorphous regions of 0.245, and an intrinsic T_1 for the crystalline regions of 1.34 s. If we try varying the percentage crystallinities that are used by a small amount, we find that while the result for the intrinsic T_1 of the amorphous regions is quite stable, the result for the intrinsic T_1 of the crystalline regions varies widely. This shows that the method can return reasonably accurate values for the active (shorter) relaxation component, but cannot give reliable values for the longer component, which contributes very little to the observed relaxation.

We return now to consider the origin of the bi-exponential T_1 behaviour. It is reasonably certain that we can ignore the possibility that the two components arise directly from the crystalline and amorphous regions, since the lamellar thicknesses present in commercial polypropylene are only of the order of a few tens of angstroms, so averaging due to spin-diffusion will be complete on the T_1 timescale. One possible explanation is that the intrinsic T_1 s of the regions are inherently not single-exponential, because of the constrained nature of the molecular motions. A second possibility is that different regions of the sample have different percentage crystallinities, for reasons which we do not yet understand, and that each of these regions exhibits a T_1 which is the population-weighted average of the crystalline and amorphous lamellae within it. This would require that these regions of differing crystallinity were sufficiently large that spin-diffusional averaging was ineffective between them (greater than several hundred angstroms, in the smallest dimension).

These two possibilities should be distinguishable, since if the T_1 is intrinsically not single-exponential then the relative proportions of the components in the FID should remain constant as a function of the time following inversion, whereas if there are domains of different crystallinity, with each giving rise to a single exponential T_1 , then the relative proportions of components in the FID should vary as a function of the time following inversion (see *Figure 2*). We carried out a series of experiments for both samples by analysing the FID at times up to 0.5 s after inversion. In these analyses, we fixed all the 'shape' parameters to their previously determined values, and allowed only the populations of the components to vary. The results clearly showed variation in the relative proportions of the components, indicating the presence of domains of different crystallinity. We decided to see if we could satisfactorily represent the data by using the simplest possible model, i.e. two independent domains with each having a defined percentage crystallinity. During the FID analyses, some of the populations of the components were negative, but in the subsequent treatment the data were normalized by using the absolute values of the populations. The changes in the populations of the FID components as a function of time after inversion were fitted using the

following:

$$P_{i(\tau)} = [P_{iA}M_A(\tau) + P_{iB}M_B(\tau)]/M_\tau$$

where i is the i th component of the FID, $P_{iA,B}$ are the populations of the i th component in domains A and B, $M_{A,B}(\tau)$ are the magnetizations in domains A and B at time τ , and $M(\tau)$ is the total magnetization at time τ . Initial 'guesses' for the T_1 behaviour were taken from the mean of the previous two-component T_1 analyses. The raw data and fitted curves are shown in Figure 3, and the results are summarized in Table 3. Fitting was achieved 'by eye', rather than by least-squares optimization, but the fit is clearly reasonable. It is not perfect, however, since the population-weighted averages for the fitted T_1 values are somewhat lower than those derived from the data.

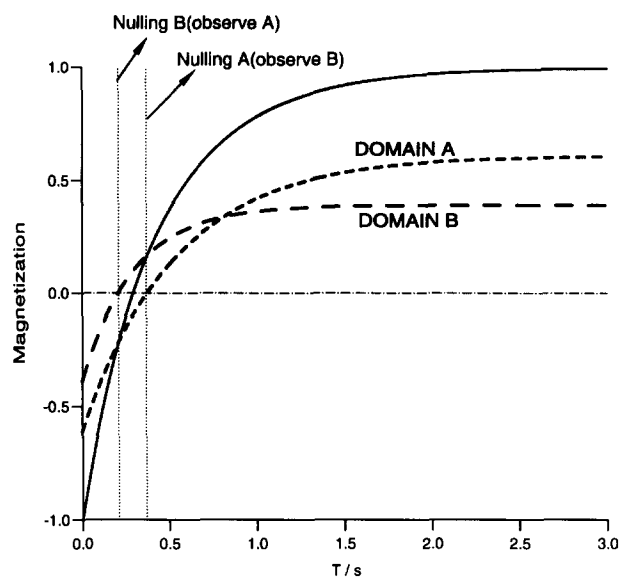


Figure 2 The inversion-nulling experiment, showing illustrative plots of magnetization of the domains as a function of the time following inversion. The parameters used were: T_1 , 0.54 and 0.30 s; t_{null} , 0.37 and 0.20 s; proportions, 61 and 39%

Nevertheless, on the basis of the T_1 values for the two domains derived from the previous analysis, we carried out an experiment in which the signal from one domain was allowed to relax to zero by waiting a time $T_1 \ln 2$ for that domain following inversion (see Figure 2), and the residual signal (from the other domain) was then flipped into the xy plane and spin-locked. In this way, it was possible to selectively measure $T_{1\rho}$ for each domain in both samples, and the results of these measurements are presented in Table 4. In each case, it was necessary to represent the decay as the sum of four exponential components. This sort of relaxation behaviour is now well understood^{14,15}, and is expected from a two-region lamellar morphology, such as semicrystalline polypropylene.

It is worth noting that the population of the longest $T_{1\rho}$ component is related indirectly to the percentage crystallinity, and that these measurements further reflect the variation in percentage crystallinity between the domains in both samples. Since the arguments presented in the Appendix are of a general nature, we can, in principle, combine the results for the percentage crystallinity in each domain (Table 3), with the population-weighted average relaxation times for each domain (obtained from Table 4) to calculate the intrinsic $T_{1\rho}$ s for the crystalline and amorphous materials. When this is

Table 3 The population (%) of each domain for polypropylene powder and granules

Component ^a	Powder		Granules	
	A	B	A	B
E	—	5	—	1
E	3	12	7	8
W	18	8	13	11
A	44	10	45	15
Total population	65	35	65	35
T_1 (s)	0.50	0.25	0.60	0.33

^a E, exponential; W, Weibullian; A, Abragamian

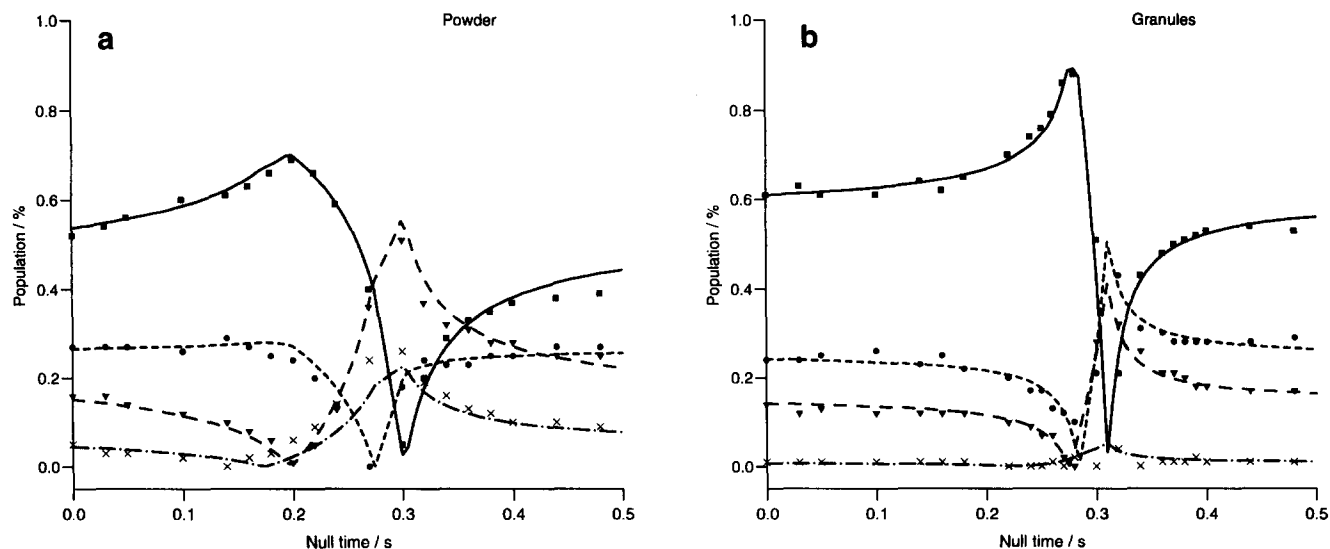


Figure 3 The relative proportions of the components in the FID as a function of nulling time for powder (a) and granules (b). The experimental points are: (■) Abragamian; (●) Weibullian; (▼, ×) the two exponentials. The computed curves (see text) are also shown

Table 4 $T_{1\rho}$ results for each domain for polypropylene powder and granules^a

Domain	$T_{1\rho}^i$ (ms)	$T_{1\rho}^{ii}$ (ms)	$T_{1\rho}^{iii}$ (ms)	$T_{1\rho}^{iv}$ (ms)
Powder A	39 ± 4 (38)	12 ± 3 (34)	1.8 ± 0.4 (18)	0.6 ± 0.2 (10)
Powder B	31 ± 2 (19)	6 ± 1 (17)	0.7 ± 0.1 (44)	0.2 ± 0.1 (20)
Granules A	33 ± 3 (35)	12 ± 3 (24)	3 ± 2 (18)	0.5 ± 0.2 (23)
Granules B	31 ± 2 (26)	7 ± 2 (23)	0.8 ± 0.2 (31)	0.3 ± 0.2 (20)

^a Figures in brackets represent populations (%)

carried out, the two samples give values of 0.37 and 0.39 ms for the intrinsic $T_{1\rho}$ of the amorphous material, but both give negative values for the intrinsic $T_{1\rho}$ of the crystalline domains. This undoubtedly reflects the limits of the analysis presented in Table 3.

CONCLUSIONS

We have shown that the combined use of FID analysis and classical relaxation measurements provides a powerful way of accessing the values of at least some of the intrinsic relaxation parameters in heterogeneous systems. An obvious extension of this approach is a two-dimensional relaxation experiment in which the complete FIDs are collected as a function of some relaxation delay, and the whole data set is then fitted simultaneously. This would both increase the effective signal-to-noise ratio, and constrain the fitting more effectively.

We have also shown that the commercial samples of polypropylene which we have been investigating contain a spatially resolved distribution of crystallinities, which can be represented to a good approximation in terms of a two-domain model.

ACKNOWLEDGEMENTS

We thank ICI Chemicals and Polymers for providing the samples that were used in this study, and for their support of this and other related work. We are also grateful to A. Bunn and N. J. Clayden for their interest in this project.

REFERENCES

- 1 Wilson, C. W. and Pake, G. E. *J. Polym. Sci.* 1953, **10**, 503
- 2 Harris, R. K., Kenwright, A. M., Royston, A. and Say, B. J. *Meas. Sci. Technol.* 1990, **1**, 1304
- 3 McDonald, M. P. and Ward, I. M. *Proc. Phys. Soc.* 1962, **80**, 1249
- 4 Powels, J. G. and Strange, J. H. *Proc. Phys. Soc.* 1963, **82**, 6
- 5 Nedler, J. A. and Mead, R. *Comput. J.* 1965, **7**, 308
- 6 Marquardt, D. W. *J. Soc. Ind. Appl. Math* 1963, **11**, 431

- 7 Press, W. H., Flannery, B. P., Teukolsky, S. A. and Vetterling, T. 'Numerical Recipes—The Art of Scientific Computing', Cambridge University Press, Cambridge, 1986, p. 506
- 8 Kenwright, A. M. and Say, B. J. in 'NMR Spectroscopy of Polymers' (Ed. R. N. Ibbett), Chapman and Hall, London, 1993, p. 246
- 9 Abragam, A. 'Principles of Nuclear Magnetism', Oxford University Press, Oxford, 1961, p. 120
- 10 Weibull, W. *J. Appl. Mech.* 1951, **18**, 293
- 11 Brereton, M. G. *J. Chem. Phys.* 1991, **94**, 2136
- 12 Brereton, M. G., Ward, I. M., Boden, N. and Wright, P. *Macromolecules* 1991, **24**, 2068
- 13 Smith, P. W. R. *PhD Thesis* University of East Anglia, 1986
- 14 Kenwright, A. M., Packer, K. J. and Say, B. J. *J. Magn. Reson.* 1986, **69**, 426
- 15 Booth, A. D. and Packer, K. J. *Mol. Phys.* 1987, **62**, 811

APPENDIX

It has been shown¹⁵ that the spin-lattice relaxation behaviour of a two-region system coupled by spin diffusion can be represented by a small number of exponential components. In such a case, where the fit is a truly adequate representation of the data, the sum of the fitted populations must equal the initial population of the magnetization, and it follows that the population-weighted relaxation rate average of the fitted components must equal the initial rate of decay of the magnetization (otherwise the fit is not an adequate representation of the data!).

In a normal spin-lattice relaxation measurement (in either the laboratory or rotating frames), the measurement starts from a condition of uniform perturbation from equilibrium, which is to say that great care must be taken so that immediately following the perturbation the magnetization population is the same in both regions of the two-domain sample. This being the case, it follows that there can be no influence of spin-diffusion between regions immediately following the perturbation, since there can be no population difference to drive the spin-diffusion. This can be seen by considering the general diffusion/relaxation equation which describes the behaviour of such systems¹⁴. This is of the form:

$$\frac{dM_{x,t}}{dt} = \frac{d}{dx} \left(D_i \frac{dM_{x,t}}{dx} \right) + \left(\frac{M_e - M_{x,t}}{T_i} \right)$$

For a relaxation starting from a spatially uniform non-equilibrium magnetization profile at $t=0$, $dM_{x,0}/dx=0$. Therefore, the term containing the diffusion coefficient drops out, and the initial magnetization decay immediately following perturbation is due solely to the intrinsic relaxation properties of the two regions, with the initial rate of decay being given by the population-weighted rate average of the intrinsic relaxation processes.

Thus, we have shown quite generally that for multi-component relaxation in such a system the population-weighted rate average of the fitted components must be equal to the population-weighted rate average of the intrinsic relaxation processes in the two regions. It can be shown mathematically that this reasoning can be generalized to systems having more than two regions.